Kisha Nandini Sivanathan, Stan Gronthos, Shane T. Grey, Darling Rojas-Canales, and Patrick T. Coates

Immunodepletion and hypoxia preconditioning of mouse vompact bone cells as a novel protocol to isolate highly immunosuppressive mesenchymal stem cells

Stem Cells and Development, 2017; 26(7):512-527

Stem Cells and Development

DOI: 10.1089/scd.2016.0180

TITLE

Immunodepletion and hypoxia preconditioning of mouse compact bone cells as a novel protocol to isolate highly immunosuppressive Mesenchymal Stem Cells

RUNNING TITLE

Suppression of compact bone generated Mesenchymal Stem Cells

AUTHORS

Kisha Nandini Sivanathan[1,2],Stan Gronthos[3,4],Shane T. Grey[5], Darling Rojas-Canales[1,2¥]

Patrick T. Coates [1,2,6¥]

[1]School of Medicine, Faculty of Health Sciences, University of Adelaide, South Australia, Australia; [2]Centre for Clinical and Experimental Transplantation, Royal Adelaide Hospital, Adelaide, South Australia, Australia; [3]South Australian Health and Medical Research Institute, Adelaide, South Australia, Australia; [4]Mesenchymal Stem Cell Laboratory, School of Medicine, Faculty of Health Sciences, University of Adelaide, South Australia, Australia; [5]Transplant Immunology Group, Garvin Institute of Medical Research, Sydney, New South Wales, Australia; [6]Central Northern Adelaide Renal Transplantation Service, Royal Adelaide Hospital, Adelaide, South Australia, Australia

[¥]D.R.C and P.T.C. contributed equally to this paper and share senior authorship.

AUTHORS DETAILS

Dr. Kisha Nandini Sivanathan

Adelaide Medical School, Faculty of Health and Medical Sciences, University of Adelaide 5005, South Australia, Australia; Centre for Clinical and Experimental Transplantation, Royal Adelaide Hospital, Adelaide 5000, South Australia, Australia.

Phone: +618-8222-0974; Fax: +612-9295-8404

Email: kisha.sivanathan@adelaide.edu.au

Professor Stan Gronthos

Mesenchymal Stem Cell Laboratory, Adelaide Medical School, Faculty of Health and Medical Sciences, University of Adelaide 5005, South Australia, Australia. South Australian Health and Medical Research Institute, Adelaide 5000, South Australia, Australia.

Phone: +618-8128-4395; Fax: +618-8313-5384

Email: stan.gronthos@adelaide.edu.au

Professor Shane T. Grey

Transplant Immunology Group, Garvan, Institute of Medical Research, Sydney, New South Wales 2010, Australia.

Phone: +619-295-8104; Fax: +612-9295-8404

Email: s.grey@garvan.org.au

Professor Patrick T. Coates

Adelaide Medical School, Faculty of Health and Medical Sciences, University of Adelaide 5005, South Australia, Australia; Centre for Clinical and Experimental Transplantation, Royal Adelaide Hospital, Adelaide 5000, South Australia, Australia; Central Northern Adelaide Renal Transplantation Service, Royal Adelaide Hospital, Adelaide, South Australia, Australia.

Telephone: 618-8222-0900; Fax: 618-8222-0957

Email: toby.coates@health.sa.gov.au

Dr. Darling Rojas-Canales[1,2¥]

Adelaide Medical School,, Faculty of Health and Medical Sciences, University of Adelaide 5005, South Australia, Australia; Centre for Clinical and Experimental Transplantation, Royal Adelaide Hospital, Adelaide 5000, South Australia, Australia.

Phone: +618-8222-0976; Fax: +612-9295-8404

Email address: Darling.Rojas@sa.gov.au

CORESSPONDING AUTHOR:

Kisha N. Sivanathan, School of Medicine, Faculty of Health Sciences, University of Adelaide, South Australia, Australia, 5005. Telephone: +618-8222-0974; Fax: +612-9295-8404; Email: kisha.sivanathan@adelaide.edu.au

ABBREVIATIONS

BM – bone marrow

CB – compact bones

CFU-F – colony forming-unit fibroblasts

mMSC – mouse mesenchymal stem cells

mMSC-17 – mouse IL-17A treated mesenchymal stem cells

UT-MSC – untreated mesenchymal stem cells

HSC – hematopoietic stem cells

MLR – mixed lymphocyte reaction

ABSTRACT

Compact bones (CB) are major reservoirs of mouse mesenchymal stem cells (mMSC). Here, we established a protocol to isolate MSC from CB and tested their immunosuppressive potential. Collagenase type II digestion of BM-flushed CB from C57B/6 mice was performed to liberate mMSC precursors from bone surfaces to establish nondepleted mMSC. CB cells were also immunodepleted based on the expression of CD45 (leukocytes) and TER119 (erythroid cells) to eliminate hematopoietic cells. $CD45^{-}TER119^{-}$ CB cells were subsequently used to generate depleted mMSC. CB nondepleted and depleted mMSC progenitors were cultured under hypoxic conditions to establish primary mMSC cultures. CB depleted mMSC compared to nondepleted mMSC showed greater cell numbers at sub-culturing and had increased functional ability to differentiate into adipocytes and osteoblasts. CB depleted mMSC had high purity and expressed key mMSC markers (>85% Sca-1, CD29, CD90) with no mature hematopoietic contaminating cells (<5% CD45, CD11b) when sub-cultured to passage 5 (P5). Nondepleted mMSC cultures however were less pure and heterogenous with <72% $Sca\text{-}1^{+}$, $CD29^{+}$ and $CD90^{+}$ cells at early passages (P1 or P2), as well as high percentages of contaminating $CD11b^{+}$ (35.6%) and $CD45^{+}$ (39.2%) cells that persisted in culture long-term. Depleted and nondepleted mMSC nevertheless exhibited similar potency to suppress total ($CD3^{+}$), $CD4^{+}$ and $CD8^{+}$ T cell proliferation, in a dendritic cell allostimulatory one-way mixed lymphocyte reaction. CB depleted mMSC, pre-treated with proinflammatory cytokines IFN-γ, TNF-α and IL-17A, CB depleted mMSC showed superior suppression of $CD8^{+}$ T cell, but not $CD4^{+}$ T cell proliferation, relative to untreated-mMSC.

In conclusion, CB depleted mMSC established under hypoxic conditions and treated with selective cytokines represents a novel source of potent immunosuppressive MSC. As these

cells have enhanced immune modulatory function, they may represent a superior product for use in clinical allotransplantation.

Keywords: compact bone mesenchymal stem cells, immunosuppression, hypoxia, proinflammatory cytokines, T cells, immunodepletion

INTRODUCTION

The bone marrow (BM) is comprised of a heterogeneous population of stem or progenitor cells including the haematopoietic stem cells (HSC), endothelial progenitor cells and mesenchymal stem cells (MSC) [1,2]. HSC are most prevalent in the bone marrow and give rise to cells of myeloid and lymphoid lineages [1]. Multipotent MSC were initially described by Friedenstein and colleagues (1970) as a rare fraction of bone marrow cells (0.001 - 0.01%) in rodents that have *in vitro* clonogenicity potential (colony forming-unit fibroblast; CFU-F) with self-renewal capacity and are able to form mineralized bone tissues under osteogenic inductive conditions [3].

The exact mechanisms by which human BM-derived MSC function *in vivo*, the route, dose and timing of MSC patient infusion as well as safety concerns with regards to MSC, off target effects, tumorgenicity [4-7] and differentiation into other cell types [8-10] remain unresolved. Together these issues limit the wide application of human BM MSC therapy into the clinic. Therefore, preclinical mouse models are widely utilized to address these issues associated with MSC therapy.

Human BM-derived MSC compared to their mouse MSC (mMSC) counterparts have been isolated and expanded *ex vivo* with high purity [11]. The rarity of mMSC from the BM however represents a major obstacle for research aiming to dissect mechanisms of MSC function *in vivo*, optimize therapeutic strategies and address safety concerns of BM MSC therapy. Mouse MSC have an extremely low incidence in BM compared to human MSC, and require modified growth conditions and media supplements for *ex vivo* expansion [12,13]. The major challenge in BM mMSC isolation protocols is to obtain a homogenous and highly purified population of mMSC, with less contaminating haematopoietic cells and other non-MSC cells or progenitor populations that co-exist in the BM niche [12-14]. Previous attempts

to eliminate these contaminating cells in mMSC cultures included immunodepletion and (or) unique culture systems such as frequent media change, low cell density cultures, alteration to the standard mMSC culture media components or cell culture surfaces to promote mMSC adherence [15-21]. Despite these attempts, isolation of mMSC from whole BM remained problematic due to poor yields or purity [21-23]. Absence of standardisation in BM mMSC isolation protocols may be a contributing factor to the conflicting results on the *in vivo* therapeutic efficacy of mMSC in preclinical mouse models of diseases including allotransplantation.

Most *in vivo* studies on the immunosuppressive function of MSC in preclinical murine models of allotransplantation use the traditionally isolated plastic-adherent selected BM mMSC [24-28], which contain numerous accessory cell populations. In this study, we established a protocol to enrich a highly purified and homogenous population of compact bone (CB) mMSC with potent *in vitro* immunosuppressive capacity that would be beneficial in an allotransplant setting. We employed collagenase type II digestion of BM depleted CB combined with immunodepletion of CD45 (lymphocyte common antigen) and TER119 (erythroid lineages) expressing cells and hypoxia preconditioning to establish primary mMSC cell lines. CB depleted mMSC were easily isolated from $CD45^-$ $TER119^-$ CB progenitor cells with higher initial cell yields at passage 1 (P1). Based on this isolation protocol, CB mMSC were also able to potently suppress *in vitro* total T cells and subset ($CD4^+$ and $CD8^+$) T cell proliferation in dendritic cells (DC) allostimulatory one-way mixed lymphocyte reaction (MLR), that mimic an *in vivo* allotransplant rejection response.

MATERIALS AND METHODS

Animals

All experimental procedures were approved by the Animal Ethics Committee of the University of Adelaide and conform to the guidelines established by the Australian Code of Practice for the Care and Use of Animals for Scientific Purposes (ethics approval M-2013-033).

Mouse MSC

Dissection of hind limbs: mMSC were isolated from BM or CB (tibia and femur) of C57BL/6 mice (4-8 mice per mMSC isolation, 6-7 weeks old). Animals were humanely killed by carbon dioxide or isoflurane overdose followed by cervical dislocation. Tibia and femur were dissected from the hind limbs in a laminar flow hood using sterile instruments and washed thoroughly with cold α-MEM (50U/ml Penicillin / 50µg/ml streptomycin). Limbs were bisected by cutting through the knee joint. Muscle and connective tissues from bones were removed by scrapping the diaphysis of the bone, then pulling the tissue towards the end of the bone. The ends of the marrow cavity were then bisected and bones were stored in cold α-MEM on ice until further processing.

Harvesting BM cells from the tibia and femur: BM cells were harvested using a 21-gauge needle, inserted into the distal end of the femur or tibia. 5 – 10ml 5% FBS/HBSS was drawn through the marrow cavity and then rapidly flushed out into the tube. This process was repeated until the bone became completely white indicating that all marrow cells have been harvested. The resulting cell suspension was passed through a 70µm nylon cell strainer to remove bone spicules or muscle and cell clumps. The viability and yields were determined by

trypan blue exclusion assay. Approximately $70x10^6$ bone marrow cells can be obtained from each mouse donor.

Mouse MSC isolation from CB: CB was crushed into small pieces (1-2mm) using a sterile blade, allowing for subsequent enzymatic digestion to release maximum number of cells. CB cells were then incubated with collagenase (at varying concentrations) and DNase I (50U/ml) for 1-2hr at 37^{o}C on a shaking platform at 240rpm. The resultant cell suspension (nondepleted mMSC precursors) was strained using a 70µm nylon cell strainer and bone chips were discarded. To isolate CB depleted mMSC, mouse CB cells were further purified using the EasySep^{TM} Mouse Mesenchymal Progenitor Enrichment Kit (StemCell Technologies; catalogue #19771) according to the manufacturer's instructions. CB cells were depleted of cells of haematopoietic origin using antibodies against CD45 and TER119. Nondepleted ($5x10^5$ cells/cm^2) and depleted ($1x10^4$ cells/cm^2) CB cells were seeded in tissue culture flasks to establish the primary CB mMSC cells lines in primary MSC media containing α-MEM, 20% (v/v) heat inactivated fetal bovine serum, 2mM L-glutamine (Multicel, USA), 1mM sodium pyruvate (Sigma Aldrich), 100µM L-ascorbate-2-phosphate, 50U/ml penicillin and 50µg/ml streptomycin [29]. Primary CB depleted or nondepleted mMSC cell lines were established at 37^{o}C in a hypoxic environment (5% O_2, 10% CO_2, 85% N_2) in a hypoxia chamber or under normoxic conditions (21% O_2), with media change performed every 2 days. At 70-80% confluence, adherent mMSC were detached using 0.25% trypsin/EDTA (Sigma) for 4min at 37^{o}C. Mouse MSC were re-seeded for expansion at a density of $1x10^4$ cells/cm^2 in tissue culture flasks and maintained in MSC media containing 10% heat inactivated FBS. Mouse MSC growth culture conditions were optimized using different batches of FBS. The effect of different FBS on nondepleted mMSC progenitor cell enrichment as well as in mMSC morphology and growth potential following mMSC sub-culturing were tested. The three FBS batches examined included: (1) SAFC Batch #10C126

(SAFC) – previously used in mMSC isolation protocols, (2) Invitrogen Batch #1153562 (Invitrogen) – new non-MSC qualified FBS and (3) Invitrogen Batch #981394 (Invitrogen MSC) –new human MSC qualified FBS. BM cell harvested from 8 mice were seeded into a T-75 flask and primary BM mMSC cell lines were established at 37^{o}C in normoxic conditions.

Mouse MSC characterisation

MSC precursors form fibroblast colony-forming unit (CFU-F) when cultured *in vitro* [30,31]. For CFU-F assays, BM or depleted CB cells were plated in a 6-well plate with primary MSC media in triplicate wells at 1x10^5 cells/well or 9x10^5 cells/well for 5 days. Cells were incubated at 37^{o}C in a humidified tissue culture incubator under normoxic (21% O_2) or hypoxic conditions (5% O_2). Nuclei of cells were stained with Toluidine blue stain and colonies were counted under an inverted light microscope (Olympus CKX41). A colony was defined as a cluster of $\geq$ 50 cells. Cobblestoned shaped colonies were excluded for CFU-F counts. Immunophenotype of culture expanded CB depleted and nondepleted CB mMSC were characterised by flow cytometry [32] (Table 1). Samples were acquired on BD FACSCantoII (BD Biosciences) flow cytometer and analysed on FCS express V4. CB mMSC were induced to differentiate into adipocytes and osteocytes as published [11]. Mouse MSC at passages 3 to 6 were used in experiments.

Cytokine treatment of CB mMSC

CB depleted mMSC (5x10^5 cells) were seeded into a T-75 tissue culture flask. Cells were allowed to adhere overnight and replaced with fresh MSC media with either no cytokines or with recombinant mouse cytokines IL-17A (50ng/ml; eBioscience), IFN-γ (500U/ml, Peprotech) and (or) TNF-α (20ng/ml, Peprotech) [33].

Dendritic cells

DC were isolated and propagated from BALB/c mice BM precursors for 5 days in RPMI 1640 medium supplemented with 10% FBS, β-mercaptoethanol (2μL/500ml), 1000U/ml recombinant mouse granulocyte macrophage colony-stimulating factor (GM-CSF; R&D Systems) and 500U/ml recombinant mouse IL-4 (R&D Systems) as previously described [34-36]. On day 5, 200ng/ml lipopolysaccharide (LPS; Sigma) was added to the BM-DC culture for 24hr to induce DC maturation. $CD11c^+$ mature DC (mDC) were positively selected using the EasySep™ mouse CD11c positive selection kit II (StemCell Technologies; catalogue #18780A) according to the manufacturer's instructions. Purified $CD11c^+$ mDC expressed mDC markers (>90% CD11b, CD11c, CD40, CD80, CD83 and CD86 and MHC class II).

Mouse T cells

Splenic $CD3^+$ T cells were isolated from C57BL/6 mice using the Mouse T cell Enrichment Column (R&D Systems; MTCC-5/10) according to the manufacturer's instructions (>90% purity). Purified $CD3^+$ T cells were labelled with carboxyfluorescein succinimidyl ester (CFSE; Invitrogen) for mouse T cell proliferation assays as per manufacturer's instructions. T cells ($10x10^6$ cells/ml) were stained with 0.7μl CFSE per 1ml cell suspension.

Mixed lymphocyte reaction (MLR)

Irradiated depleted or nondepleted mMSC (30 Grays) at $1x10^2$ (0.1%), $1x10^3$ (1%) or $1x10^4$ cells (10%) were seeded overnight into 96-well round bottom plates in a total volume of 0.2ml complete RPMI 1640 medium. CFSE-labelled responder $CD3^+$ T cells ($1x10^5$cells) and 30 Grays irradiated stimulator mDC ($1x10^4$cells) at a DC to T cell ratio of 1:10. Cells were cultured for 3 or 5 days and T cells were harvested for analysis of CFSE-labelled T cell

proliferation. Harvested CFSE-labelled T cells were also cell-surface stained with anti-CD4 and anti-CD8 antibodies to detect proliferation levels of $CD4^+$ and $CD8^+$ T cells, respectively (Table 1).

Statistics

Statistical significances ($p<0.05$) were assessed by one- or two- analysis of variance (ANOVA) with post-Sidak multiple comparison tests or Kruskal-Wallis with post-Dunn multiple comparison tests. Statistical analyses were performed using the GraphPad Prism software (GraphPad Software, LA Jolla, CA, http://www.graphpad.com/).

RESULTS

Optimization of compact bone mMSC isolation and culture

We aimed to establish a protocol to enrich and isolate a highly purified and homogenous population of CB mMSC. Collagenase digestion is an essential step to isolate mMSC progenitors from CB. CB derived Sca-1^+ cells (stem cell antigen-1) are previously known to be precursor cells of mMSC [37-39], providing an indication if the bone digestion step was sufficient to release mMSC precursors from the CB. Collagenase II (3mg/mL, 1 hr) resulted in high yield of CB cells and the highest of Sca-1^+ cells (34.66%) immediately after CB digestion compared to all the other CB digestion conditions (Table 2). The colony forming efficacy of the differently digested bone fragments confirmed that the digestion protocol was sufficient to release mMSC precursor cells from CB, where collagenase II (3mg/mL, 1 hr) showed the highest CFU-F efficacy with low toxicity (>90% viability).

FBS batches vary in quality and composition. This may affect adherence, mitotic expansion of primary MSC cultures as well as the retention of MSC in undifferentiated states [40]. All FBS batches showed no difference in the enrichment of mMSC progenitor cells evident by the comparable number of CFU-F in primary mMSC cultures and no aberrant changes in mMSC morphology (Figure 1A,B). Invitrogen FBS was optimal for mMSC cultures as it favoured mMSC growth, particularly from P2 to P3 when compared to Invitrogen MSC FBS (Figure 1C) and was subsequently used in all mMSC isolations and cultures.

Hypoxic culture conditions favoured the enrichment and growth of mMSC progenitor cells evident by the high numbers of CFU-F derived from these CB cells (Figure 1A, Table 3). Precursors of mMSC were highly prevalent in the CB rather than in the bone marrow fraction as CB derived mMSC had higher colony forming efficiency (Figure 1A).

Based on the optimization of culture conditions of CB nondepleted mMSC isolation, we have established a protocol to maximize the enrichment and expansion of mMSC. Collagenase II (1hr, 3mg/ml) digestion of the CB followed by hypoxia culture, isolated, selected and enhanced the clonogenicity of CB derived mMSC precursors. This protocol was used as a standard operating procedure for the culture and establishment of nondepleted and depleted mMSC cell lines from CB precursors. Depleted mMSC cell lines were established using these culture conditions in addition to lineage depletion of CD45 (lymphocyte common antigen) and TER119 cells (erythroid lineages) of the digested CB fragments with the aim to isolate highly pure CB mMSC precursors compared to nondepleted mMSC.

CD45 and TER119 depletion of compact bone cells enhances mMSC precursor enrichment

CB depleted mMSC precursors obtained following CD45 and TER119 immunodepletion represented only a very small fraction (0.02 – 1%) of the digested CB cells. Following 5 days of culture under hypoxia with media change every 2 days, there was a 5.9-fold increase in the numbers of CB depleted mMSC when subcultured from P0 to P1 (Figure 2C). Nondepleted mMSC precursors were initially seeded at a 50x higher seeding density to obtain comparative density and growth rates as observed with depleted mMSC at day 5 under hypoxia. There was however a decrease in cell numbers at P0 to P1 due to the low frequency of mMSC precursors in the CB nondepleted fraction (Figure 2C). There was also presence of cells with a cobblestoned appearance, that contaminated the nondepleted mMSC cultures, whereas depleted mMSC cultures showed homogeneity of cell morphology, exhibiting a fibroblastic MSC-like appearance as early as P0 and P1 (Figure 2B). CB depleted also showed highest enrichment of Sca-1^{+} cells (90.6% ± 1.141) and were homogenous in Sca-1 expression,

compared to CB nondepleted mMSC (72.4% ± 3.635) at P1 (Figure 2A). The level of Sca-1 expression was also highest in CB depleted mMSC (Figure 2A).

Additionally, both depleted and nondepleted mMSC showed similar increase in fold proliferation from P1 to P4 (Figure 2C). Nondepleted mMSC however had reduced proliferation potential when sub-cultured to higher passages (P4 to P5; 1.5-fold) and when compared to depleted mMSC (3.0-fold).

Interestingly, BM mMSC initially established under normoxia at the highest seeding density with frequent media change exhibited lowest Sca-1 percentages (18.0% ± 5.083) and expression levels (Figure 2A). BM mMSC cultures were heterogenous with cobblestone colonies, round adherent cells and cells were less elongated and fibroblastic-like (Figure 2B). Culture of BM mMSC was unsuccessful as they failed to proliferate beyond P1 and was therefore not used in this study.

CB depleted mMSC have high purity and greater functional differentiation potential

In subsequent experiments, we further compared and characterised the immunophenotype and differentiation potential of CB nondepleted and depleted mMSC. At a low passage (P2), depleted mMSC cultures had higher percentages of cells expressing key MSC markers Sca-1 (94.3%), CD29 (85.0%) and CD90 (86.7%) compared to nondepleted mMSC with 71.4%, 54.2% and 63.2% positive cells, respectively (Figure 3A). Sca-1 was also highly expressed by depleted mMSC relative to nondepleted mMSC at P2. Nondepleted mMSC at a higher passage (P5) nevertheless showed increased percentages of Sca-1^+ and $CD90^+$ when compared to P2 and were similar to depleted mMSC. Other standard positive MSC markers CD44 and CD105 were expressed similarly by both mMSC groups regardless of the passage.

Early nondepleted mMSC cultures (P2) were contaminated with $CD11b^+$ (35.6%) and $CD45^+$ (39.2%) cells expressing high levels of these markers (Figure 3B). The

percentages and the expression levels of CD11b (20.8%) and CD45 (10.3%) decreased in nondepleted cultures upon sub-culturing. Low and high passage depleted mMSC had <5% contaminating $CD11b^+$ and $CD45^+$ cells. Depleted mMSC also exhibited higher functional capacity and could differentiate more efficiently into adipocytes and osteoblasts (Figure 4A). The high intensity of Alizarin Red staining indicated increased number of osteocytes containing calcium deposit in depleted mMSC. Similarly, greater lipid formation detected by Oil Red O staining suggested the enhanced differentiation capacity of depleted mMSC into adipocytes (Figure 4A).

Depleted and nondepleted mMSC exhibited comparable inhibition of T cell proliferation

Nondepleted and depleted mMSC inhibited allogeneic DC stimulated T cell proliferation in a dose-dependent manner at days 3 and 5 of the MLR assay with similar efficacy (Figure 4B). Maximal immunosuppression of T cells was observed at 10% mMSC dose whereby $CD4^+$ T cell proliferation was suppressed by up to 83.4% and 81.2% at days 3 and 5 of MLR, respectively, while $CD8^+$ T cell proliferation was inhibited by up to 86.5% and 82.6% (Figure 4B cumulative data; Table 4). Both nondepleted and depleted mMSC retained their immunosuppressive capacity on total, $CD4^+$ and $CD8^+$ T cells when used at lower doses (1% or 0.1%).

CB depleted mMSC-17 are not superior suppressors of T cells

We have previously established that human IL-17A pre-treated MSC (MSC-17) conformed to untreated MSC (UT-MSC) immunophenotype and are superior suppressors of T cells [33]. Since CD45 and TER119 depletion of CB cells yields a highly purified and homogenous population of mMSC compared to nondepleted mMSC, subsequent experiments were

conducted using only depleted mMSC. Here, we aimed to determine if murine CB depleted mMSC treated with IL-17A (mMSC-17) have similar characteristics to human MSC-17 and retained UT-MSC phenotype. Immunophenotype of mMSC-17 was similar to untreated mMSC (UT-mMSC) following 5 days of IL-17A treatment (supplementary Figure S1, A). UT-mMSC and mMSC-17 expressed the conventional mMSC markers Sca-1, CD29, CD44, CD90 and were negative for CD11b, CD31, CD34, and CD45, with no difference in expression levels between UT-mMSC and mMSC-17. Both UT-mMSC and mMSC-17 retained their functional capacity and could differentiate into adipocytes and osteoblasts (supplementary Figure S1, B). Additionally, mMSC-17 did not exhibit enhanced proliferation compared to UT-mMSC (supplementary Figure S1, C). Surprisingly, we identified that CB mMSC had protein expression of the IL-17 receptor IL-17RC but not IL-17RA (supplementary Figure S1, A). Unexpectedly, when mMSC were treated with IL-17A for 5 days prior to use in the MLR, no enhancement of T cell immunosuppression was observed in the mMSC-17 groups compared to UT-mMSC (supplementary Figure S2). The effect of 3 days IL-17A treatment of mMSC was also investigated. However, no significant differences in suppression of T cell proliferation were observed between UT-mMSC and mMSC-17 (data not shown).

TNF-α enhances the immunosuppressive effect of CB depleted mMSC

MSC pre-treated with other inflammatory cytokines including IFN-γ and TNF-α as well as in a cytokine combination cocktail have previously been shown to enhance MSC immunosuppression [33,41,42]. Hence, we further explored the capacity of 5 day IFN-γ (MSC-γ), and TNF-α (MSC-TNF) treated mMSC on T cell suppression. MSC-γ showed no improvement in MSC inhibition of T cells, comparable to UT-MSC. Interestingly, CB

depleted MSC-TNF exhibited most potent suppression on allogeneically activated $CD8^+$ T cells at day 5 MLR by 92.6% (Figure 5).

We also investigated if IL-17A could act synergistically with either IFN-γ (MSC-γ/17) or TNF-α (MSC-TNF/17) or in combination of both IFN-γ and TNF-α (MSC-γ/TNF/17) to enhance mMSC immunosuppression. Although MSC-TNF/17 augmented mMSC inhibition on $CD8^+$ T cells relative to UT-MSC by 3.2-fold, no additional T cell suppression was observed with respect to mMSC treated with TNF-α alone (MSC-TNF) (Figure 5B). MSC-γ/17/TNF were most potent amongst all other cytokine pre-treatment at suppressing $CD8^+$ T cell proliferation at day 3 and 5 MLR, by 2.3- and 4.2-fold, respectively (Figure 5A,B). MSC-γ/TNF/17 were also superior to UT-MSC at inhibiting total T cell proliferation at day 5 MLR (Figure 5B). The enhancement of T cell immunosuppression by MSC-TNF, MSC-TNF/17 and MSC-γ/TNF/17 was only evident with high mMSC doses (10%) (Figure 5B, supplementary Figure S3). It should be noted that TNF-α in mMSC cultures drastically altered MSC morphology, changing their fibroblastic-like appearance to a hypertrophic flattened irregular shape. TNF-α also significantly inhibited mMSC growth potential (data not shown).

DISCUSSION

In this study, we have shown that compact bones (CB) have emerged to be one of the major reservoirs of clonogenic MSC or progenitor cells in the murine system [22,23,37,43]. The stem cell antigen-1 (Sca-1) has recently emerged as a potential marker to isolate mMSC precursors with higher clonogenicity potential, cell yields and to maintain CB mMSC in an undifferentiated state [37-39]. Precursors of mMSC were mostly prevalent in the CB rather than in the bone marrow fraction as CB derived mMSC had higher colony forming efficiency and percentages of highly expressing Sca-1^+ cells, indicating greater enrichment of mMSC. Mouse MSC are traditionally isolated from the BM but mMSC are present at low frequencies where BM mMSC preparations are highly heterogeneous with many contaminating haematopoietic cells, monocytes, granulocytes and pre-B cell progenitors that co-adhere with BM mMSC cultures [12,13,21,44]. We also observed the presence of colonies with various morphologies including less elongated and fibroblastic-like-MSC colonies as well as cells with cobblestoned appearance; confirming the heterogeneity of the primary BM mMSC cultures.

BM mMSC compared to CB nondepleted and depleted mMSC also exhibited low growth kinetics and failed to be maintained in *in vitro* tissue culture conditions beyond passage 1 (P1), despite the high seeding density to initially establish the BM mMSC cell lines. BM mMSC cultured under atmospheric oxygen (21% O_2; normoxia) where shown to induce the expression of p53 and mitochondrial reactive oxygen species in mMSC [45]. These molecules resulted in oxidative stress, increased death and caused growth arrest of BM mMSC [45]. This may provide a plausible explanation to the failure to maintain BM mMSC propagation from whole BM beyond P1, due to long-term atmospheric oxygen exposure that resulted in cell growth arrest. Low oxygen tension (2% or 5% O_2) has been shown to support

BM mMSC clonogenicity and retained their multipotency [45-47]. However, data presented in this study and by other groups have shown that BM mMSC compared to their CB counterparts have lower clonogenicity potential and cell yields when established under hypoxia [39,46]. Moreover, studies using Sca-1/Ly-6A null mice suggest that Sca-1 is required for the regulation of mesenchymal progenitor cell self-renewal [48,49]. The very low percentages and levels of Sca-1 expressing cells detected at P1 may also be a confounding factor contributing to the failed self-renewal capacity of BM mMSC in our experiments. Hence, CB derived mMSC cell lines established under hypoxia represent an alternative source to BM to isolate and enrich for a highly purified population of mMSC.

Studies exploring the use of CB derived mMSC instead of the conventional BM mMSC use different methods of isolation and culture. These studies generated CB mMSC by the culture of the whole compact bone [23], undigested CB fragments [22], collagenase digestion of CB with or without FACS sorting [37,39] or by the culture of BM-flushed digested CB fragments [43]. All these studies employed either hypoxia or normoxic culture conditions to isolate mMSC from precursor cells. In the present study, we aimed to optimize, improvise and standardize current CB mMSC isolation and culture systems. Hence, we extensively compared the enrichment, growth potential, immunophenotype, functional differentiation capacity and the immunosuppressive properties of BM-flushed collagenase II digested CB nondepleted and $CD45^-$ $TER119^-$ (depleted) mMSC that were established under hypoxia and successively passaged under normoxia.

Although lower cell yields were obtained following CD45 and TER119 depletion of CB cells, there was a substantial increase in cell numbers of depleted mMSC as to CB nondepleted cells that were seeded at a 50x higher seeding density. This was due to the extremely low frequency of CB mMSC progenitors that reside in the compact bones (0.02-1%) from whole CB digested fragments. Immunodepletion of mature hematopoietic cells

CD45 (lymphocytes) and TER119 (erythroid lineages) eliminated majority of these contaminating cells, particularly CD45 that persist in early (P2) and long-term (P5) mMSC cultures as shown in this study with nondepleted mMSC. The reduced purity and high heterogeneity of nondepleted mMSC cultures due to contaminating $CD45^+$ cells have been previously shown to persist even above P5 [23]. High frequencies of $CD45^+$ cells that co-adhere with mMSC were also evident in protocols involving the culture of whole bone fragments to enable mMSC to migrate out of the compact bones [22] as well as from collagenase digested or undigested nondepleted CB mMSC [22,39,43]. In addition, we report that nondepleted mMSC cultures also have high percentages of $CD11b^+$ cells (monocytes, NK cells, granulocytes, macrophages), consistent with another report [43]. These innate immune $CD11b^+$ cells were absent in depleted mMSC, further validating the high purity and homogenicity of depleted mMSC. $CD11b^+$ and $CD45^+$ contaminants in nondepleted mMSC can be reduced by sub-culturing, but were not eliminated by P5. This may have compromised nondepleted mMSC growth capacity at later passages as well as their reduced efficacy to functionally differentiate into adipocytes and osteoblasts in response to classical induction conditions. Reduced nondepleted mMSC growth potential also represents a significant impediment to the generation of sufficient number of cells for *in vivo* infusion. In human studies, we and others have shown that depleting blood cells from the MSC preparations results in higher MSC growth rates and differentiation potential [50]consistent with our observed results with CB depleted mMSC.

Greater enrichment of highly expressing Sca-1^+ cells (>90% positivity) were also evident in the depleted CB mMSC compared to nondepleted mMSC at early passages, P1 and P2. Early depleted mMSC cultures (P2) were also highly positive (>85%) for the expression of key mMSC markers CD29 and CD90. Nondepleted mMSC on the contrary exhibited a heterogenous population of cells that were CD29 and CD90 positive (<64%), whilst also

having a negative cell fraction for these markers. These data suggest that CD45 and TER119 immunodepletion of CB progenitors improves CB mMSC enrichment, resulting in highly pure and homogenous cell preparations.

Although adipose derived mMSC (mASC) isolations can be technically easier compared to harvesting mMSC from the bone in a murine system, MSC-like populations from different sources vary in their immunophenotype, functional differentiation potential, transcriptome and proteome profiling [51]. Different populations of MSC are also known to respond differentially in an inflammatory milieu and exert different mechanisms of immune modulation [52-54]. In preliminary studies, we performed immunophenotypic analysis of mASC isolated from epididymal fat of C57B/6 mice. Early mASC cultures established under normoxia or hypoxia expressed lower levels and percentages of Sca-1^+ cells (< 22.0%, data not shown) compared to CB mMSC (>90% Sca-1 positivity). Mouse ASC cultures like CB nondepleted mMSC were also contaminated with high percentages of hematopoietic cells CD11b (30.3%) and CD45 (33.4%) (data not shown), while CB depleted mMSC showed absence of these cells. From our experience as well as reports published by others, a large proportion of contaminating $CD34^+$ cells (30.3%) persist in early mASC cultures [55,56]. Therefore, the heterogeneity of mASC cultures, similar to CB nondepleted mMSC may limit the overall therapeutic efficacy of mASC to control alloimmune responses in preclinical models of allotransplantation rejection.

Dendritic cells (DC) are the most potent antigen presenting cells of the immune system. We isolated and generated LPS-matured DC from allogeneic bone marrow donors to be used as an antigen presenting cell to induce robust T cell proliferation. We specifically evaluated and compared the immunosuppressive properties of autologous nondepleted and depleted mMSC on total and T cell subsets ($CD4^+$ and $CD8^+$ T cells). Surprisingly, we observed no differences in the potency of nondepleted and depleted mMSC to suppress *in vitro* allogeneic DC stimulated T cell proliferation. Nonetheless, the use of a DC stimulated T cell MLR is more indicative of a mechanism by which CB mMSC may modulate T cell

responses, previously unidentified with CB mMSC in the literature. Previous studies investigating *in vitro* T cell immunosuppressive properties by CB mMSC have used nonspecific-mitogenic stimulation [43], CD3/CD28 activation of T cells [39] or allogeneic splenocytes (mixed population of stimulator cells) to induced T cell proliferation [43]. In this study, a DC-T cell MLR was used instead to more closely mimic *in vivo* mechanisms of cell-mediated antigen specific immune response to the allograft [27]. Evaluating mechanisms by which CB mMSC modulate T cell responses *in vitro* in the presence of DC warrants further investigation.

Despite the observed similarity of depleted and nondepleted CB mMSC to modulate T cell proliferation *in vitr*o, the administration of CB nondepleted mMSC as a therapy for *in vivo* allotransplantation rejection maybe limited by several factors discovered by our study. Firstly, nondepleted CB mMSC tend to have an early decline in culture with reduced mMSC proliferative capacity and secondly, a resultant heterogenous population. The contaminating innate ($CD11b^+$) and adaptive ($CD45^+$) immune inflammatory cells may trigger undesired immune responses *in vivo*, especially if allogeneic- or third-party derived mMSC are administered to prevent allotransplantation rejection. These innate and adaptive inflammatory cells may amplify immune responses associated with graft rejection, thereby reducing the therapeutic efficacy of mMSC *in vivo* through mechanisms that we extensively reviewed in a previous publication [27]. For these reasons, we further explored strategies in which we can enhance the immunomodulatory properties of CB depleted mMSC but not nondepleted mMSC.

Given that CB depleted mMSC give rise to a homogenous population with an easy expansion capacity, we conducted further experiments to explore strategies to enhance their immunomodulatory capacity. We have previously shown that proinflammatory cytokines can regulate MSC function to promote a superior immunomodulatory phenotype [33]. For

example, IL-17A (MSC-17) or IFN-γ (MSC-γ) preconditioned human BM MSC functioned as superior suppressors of T cells compared to untreated MSC (UT-MSC) [33]. Interestingly, CB depleted mouse MSC-γ and MSC-17 differed from human MSC-γ or MSC-17 as they were ineffective at enhancing suppression of allogeneically stimulated T cell proliferation compared to UT-MSC. The combination of IL-17A in a dual cytokine cocktail with either IFN-γ (MSC-γ/17) or TNF-α (MSC-TNF/17) also failed to show improvements or have an additive effect on mMSC T cell immunosuppression. Our data is consistent with another study showing that the treatment of BM mMSC with IFN-γ or IL-17 alone is ineffective at increasing the ability of mMSC to suppress T cell proliferation *in vitro* [42]. Nevertheless, in a triple cytokine combination cocktail of IFN-γ, TNF-α and IL-17A (MSC-γ/TNF/17), CB depleted mMSC were shown to be superior at suppressing total T cell proliferation at day 5 MLR, supporting findings from Han *et. al.* (2014). In addition to this previous study, we demonstrated specifically that the enhanced inhibition of CB depleted MSC-γ/TNF/17 compared to UT-MSC was evident only on the $CD8^+$ T cells but not $CD4^+$ T cells at day 3 and 5 MLR. We also report that CB MSC-TNF and MSC-TNF/17 relative to UT-MSC exhibited greater inhibition of only $CD8^+$ T cell proliferation at day 5 MLR. Mechanistically, BM derived MSC-γ/TNF/17 are known to inhibit *in vivo* Con-A induced liver injury via the induction of immunosuppressive iNOS [42]. TNF-α is also known to increase MSC adhesiveness and migration *in vitro* and *in vivo* with improvement of cardiac function recovery after myocardial infarction [57]. A latter study verified that TNF-α can induce the expression of chemotaxis molecules including CCL2 and CCL5 by MSC [42]. TNF-α in combination with IFN-γ and IL-17A pre-treated BM mMSC further upregulated CCL2 and CCL5, while inducing the expression of other chemokines such as CXCL9 and CXCL10 in mMSC [42]. The functional role of immunoregulatory iNOS and chemokines in CB depleted

mMSC in suppressing allogeneic DC-stimulated $CD8^+$ T cell proliferation remains to be elucidated.

In summary, immunodepletion and hypoxia preconditioning of mouse CB cells represent a novel protocol to isolate highly purified, homogeneous and immunosuppressive mMSC that would be beneficial in models of allotransplantation rejection and inflammatory diseases. CB depleted mMSC exhibited potent immunosuppressive effect on $CD4^+$ and $CD8^+$ T cells, which are the key effector cells mediating mechanisms of allograft rejection. We have also, for the first time shown that the immunosuppressive properties of CB depleted mMSC on DC-stimulated T cell proliferation can be amplified by preconditioning mMSC with IFN-γ, TNF-α and IL-17A. A DC-T cell MLR can be a useful system to investigate the immunomodulatory effects of MSC on T cell via the regulation of DC. In the future, we also aim to compare the therapeutic efficacy of CB nondepleted and depleted mMSC to prevent rejection and prolong allograft survival and function *in vivo* in mouse models of allotransplantation.

ACKNOWLEDGEMENTS

This work was supported by grants from The Hospital Research Foundation, The Queen Elizabeth Hospital, Adelaide, South Australia. K.N.S. We also thank Svjetlana Kireta for proof-reading this manuscript. PhD was financed by the Adelaide Graduate Research Scholarship, University of Adelaide, South Australia and The Hospital Research Foundation Scholarship.

DISCLOSURE STATEMENT

The authors declare no competing financial interests.

REFERENCES

1. Ratajczak MZ, M Kucia, M Majka, R Reca and J Ratajczak. (2004). Heterogeneous populations of bone marrow stem cells--are we spotting on the same cells from the different angles? Folia Histochem Cytobiol 42:139-46.
2. Mendez-Ferrer S, TV Michurina, F Ferraro, AR Mazloom, BD Macarthur, SA Lira, DT Scadden, A Ma'ayan, GN Enikolopov and PS Frenette. (2010). Mesenchymal and haematopoietic stem cells form a unique bone marrow niche. Nature 466:829-34.
3. Friedenstein AJ, RK Chailakhjan and KS Lalykina. (1970). The development of fibroblast colonies in monolayer cultures of guinea- pig bone marrow and spleen cells. Cell Proliferation 3:393-403.
4. Wang GQ, JR Xu, R Wang, HX Li, N Xu, XB Du and YQ Wei. (2006). [Inhibitory effect of mesenchymal stem cells carrying murine beta defensin 2 on malignant ascites in mice]. Ai Zheng 25:657-62.
5. Ren G, Y Liu, X Zhao, J Zhang, B Zheng, ZR Yuan, L Zhang, X Qu, JA Tischfield, C Shao and Y Shi. (2013). Tumor resident mesenchymal stromal cells endow naive stromal cells with tumor-promoting properties. Oncogene.
6. Nishimura K, S Semba, K Aoyagi, H Sasaki and H Yokozaki. (2012). Mesenchymal stem cells provide an advantageous tumor microenvironment for the restoration of cancer stem cells. Pathobiology 79:290-306.
7. Rosland GV, A Svendsen, A Torsvik, E Sobala, E McCormack, H Immervoll, J Mysliwietz, JC Tonn, R Goldbrunner, PE Lonning, R Bjerkvig and C Schichor. (2009). Long-term cultures of bone marrow-derived human mesenchymal stem cells frequently undergo spontaneous malignant transformation. Cancer Res 69:5331-9.

8. Breitbach M, T Bostani, W Roell, Y Xia, O Dewald, JM Nygren, JW Fries, K Tiemann, H Bohlen, J Hescheler, A Welz, W Bloch, SE Jacobsen and BK Fleischmann. (2007). Potential risks of bone marrow cell transplantation into infarcted hearts. Blood 110:1362-9.

9. Kunter U, S Rong, P Boor, F Eitner, G Muller-Newen, Z Djuric, CR van Roeyen, A Konieczny, T Ostendorf, L Villa, M Milovanceva-Popovska, D Kerjaschki and J Floege. (2007). Mesenchymal stem cells prevent progressive experimental renal failure but maldifferentiate into glomerular adipocytes. J Am Soc Nephrol 18:1754-64.

10. Prigozhina TB, S Khitrin, G Elkin, O Eizik, S Morecki and S Slavin. (2008). Mesenchymal stromal cells lose their immunosuppressive potential after allotransplantation. Exp Hematol 36:1370-6.

11. Gronthos S, ACW Zannettino, SJ Hay, S Shi, SE Graves, A Kortesidis and PJ Simmons. (2003). Molecular and cellular characterisation of highly purified stromal stem cells derived from human bone marrow. Journal of cell science 116:1827-1835.

12. Short B, N Brouard, R Driessen and PJ Simmons. (2001). Prospective isolation of stromal progenitor cells from mouse BM. Cytotherapy 3:407-8.

13. English K, A French and KJ Wood. (2010). Mesenchymal stromal cells: facilitators of successful transplantation? Cell Stem Cell 7:431-42.

14. Phinney DG, G Kopen, RL Isaacson and DJ Prockop. (1999). Plastic adherent stromal cells from the bone marrow of commonly used strains of inbred mice: variations in yield, growth, and differentiation. J Cell Biochem 72:570-85.

15. Sun S, Z Guo, X Xiao, B Liu, X Liu, PH Tang and N Mao. (2003). Isolation of mouse marrow mesenchymal progenitors by a novel and reliable method. Stem Cells 21:527-35.

16. Baddoo M, K Hill, R Wilkinson, D Gaupp, C Hughes, GC Kopen and DG Phinney. (2003). Characterization of mesenchymal stem cells isolated from murine bone marrow by negative selection. J Cell Biochem 89:1235-49.

17. Tropel P, D Noel, N Platet, P Legrand, AL Benabid and F Berger. (2004). Isolation and characterisation of mesenchymal stem cells from adult mouse bone marrow. Exp Cell Res 295:395-406.

18. Phinney DG. (2008). Isolation of mesenchymal stem cells from murine bone marrow by immunodepletion. Methods Mol Biol 449:171-86.

19. Nadri S, M Soleimani, RH Hosseni, M Massumi, A Atashi and R Izadpanah. (2007). An efficient method for isolation of murine bone marrow mesenchymal stem cells. Int J Dev Biol 51:723-9.

20. Jeon MS, TG Yi, HJ Lim, SH Moon, MH Lee, JS Kang, CS Kim, DH Lee and SU Song. (2011). Characterization of mouse clonal mesenchymal stem cell lines established by subfractionation culturing method. World J Stem Cells 3:70-82.

21. Krishnappa V, SV Boregowda and DG Phinney. (2013). The peculiar biology of mouse mesenchymal stromal cells--oxygen is the key. Cytotherapy 15:536-41.

22. Cai Y, T Liu, F Fang, C Xiong and S Shen. (2015). Comparisons of mouse mesenchymal stem cells in primary adherent culture of compact bone fragments and whole bone marrow. Stem Cells Int 2015:708906.

23. Yamachika E, H Tsujigiwa, M Matsubara, Y Hirata, K Kita, K Takabatake, N Mizukawa, Y Kaneda, H Nagatsuka and S Iida. (2012). Basic fibroblast growth factor supports expansion of mouse compact bone-derived mesenchymal stem cells (MSCs) and regeneration of bone from MSC in vivo. J Mol Histol 43:223-33.

24. Casiraghi F, N Azzollini, M Todeschini, RA Cavinato, P Cassis, S Solini, C Rota, M Morigi, M Introna, R Maranta, N Perico, G Remuzzi and M Noris. (2012).

Localization of mesenchymal stromal cells dictates their immune or proinflammatory effects in kidney transplantation. Am J Transplant 12:2373-83.

25. Takahashi T, A Tibell, K Ljung, Y Saito, A Gronlund, C Osterholm, J Holgersson, T Lundgren, BG Ericzon, M Corbascio and M Kumagai-Braesch. (2014). Multipotent Mesenchymal Stromal Cells Synergize With Costimulation Blockade in the Inhibition of Immune Responses and the Induction of Foxp3+ Regulatory T Cells. Stem Cells Transl Med.

26. Wang H, F Qi, X Dai, W Tian, T Liu, H Han, B Zhang, H Li, Z Zhang and C Du. (2014). Requirement of B7-H1 in mesenchymal stem cells for immune tolerance to cardiac allografts in combination therapy with rapamycin. Transpl Immunol 31:65-74.

27. Sivanathan KN, S Gronthos, D Rojas-Canales, B Thierry and PT Coates. (2014). Interferon-gamma modification of mesenchymal stem cells: implications of autologous and allogeneic mesenchymal stem cell therapy in allotransplantation. Stem Cell Rev 10:351-75.

28. Ben Nasr M, A Vergani, J Avruch, L Liu, E Kefaloyianni, F D'Addio, S Tezza, D Corradi, R Bassi, A Valderrama-Vasquez, V Usuelli, J Kim, J Azzi, B El Essawy, J Markmann, R Abdi and P Fiorina. (2015). Co-transplantation of autologous MSCs delays islet allograft rejection and generates a local immunoprivileged site. Acta Diabetol.

29. Hegner B, T Schaub, R Catar, A Kusch, P Wagner, K Essin, C Lange, G Riemekasten, D Dragun and CU Berlin. Deregulated vascular smooth muscle cell differentiation with increased propensity towards myofibroblastic phenoconversion of mesenchymal stem cells from patients with systemic sclerosis.

30. Owen M and AJ Friedenstein. (1988). Stromal stem cells: marrow-derived osteogenic precursors. Ciba Found Symp 136:42-60.

31. Gronthos S, SE Graves, S Ohta and PJ Simmons. (1994). The STRO-1+ fraction of adult human bone marrow contains the osteogenic precursors. Blood 84:4164-73.

32. Wada N, D Menicanin, S Shi, PM Bartold and S Gronthos. (2009). Immunomodulatory properties of human periodontal ligament stem cells. J Cell Physiol 219:667-76.

33. Sivanathan KN, DM Rojas-Canales, CM Hope, R Krishnan, RP Carroll, S Gronthos, ST Grey and PT Coates. (2015). Interleukin-17A-Induced Human Mesenchymal Stem Cells Are Superior Modulators of Immunological Function. Stem Cells 33:2850-63.

34. Inaba K, M Inaba, N Romani, H Aya, M Deguchi, S Ikehara, S Muramatsu and RM Steinman. (1992). Generation of large numbers of dendritic cells from mouse bone marrow cultures supplemented with granulocyte/macrophage colony-stimulating factor. J Exp Med 176:1693-702.

35. Morelli AE, AT Larregina, RW Ganster, AF Zahorchak, JM Plowey, T Takayama, AJ Logar, PD Robbins, LD Falo and AW Thomson. (2000). Recombinant adenovirus induces maturation of dendritic cells via an NF-kappaB-dependent pathway. J Virol 74:9617-28.

36. Morelli AE, AF Zahorchak, AT Larregina, BL Colvin, AJ Logar, T Takayama, LD Falo and AW Thomson. (2001). Cytokine production by mouse myeloid dendritic cells in relation to differentiation and terminal maturation induced by lipopolysaccharide or CD40 ligation. Blood 98:1512-23.

37. Short BJ, N Brouard and PJ Simmons. (2009). Prospective isolation of mesenchymal stem cells from mouse compact bone. Methods Mol Biol 482:259-68.

38. Houlihan DD, Y Mabuchi, S Morikawa, K Niibe, D Araki, S Suzuki, H Okano and Y Matsuzaki. (2012). Isolation of mouse mesenchymal stem cells on the basis of expression of Sca-1 and PDGFR-alpha. Nat Protoc 7:2103-11.

39. Baustian C, S Hanley and R Ceredig. (2015). Isolation, selection and culture methods to enhance clonogenicity of mouse bone marrow derived mesenchymal stromal cell precursors. Stem Cell Res Ther 6:151.

40. Lennon DP, SE Haynesworth, SP Bruder, N Jaiswal and AI Caplan. (1996). Human and animal mesenchymal progenitor cells from bone marrow: identification of serum for optimal selection and proliferation. In Vitro Cellular & Developmental Biology-Animal 32:602-611.

41. Ren G, L Zhang, X Zhao, G Xu, Y Zhang, AI Roberts, RC Zhao and Y Shi. (2008). Mesenchymal stem cell-mediated immunosuppression occurs via concerted action of chemokines and nitric oxide. Cell Stem Cell 2:141-50.

42. Han X, Q Yang, L Lin, C Xu, C Zheng, X Chen, Y Han, M Li, W Cao, K Cao, Q Chen, G Xu, Y Zhang, J Zhang, RJ Schneider, Y Qian, Y Wang, G Brewer and Y Shi. (2014). Interleukin-17 enhances immunosuppression by mesenchymal stem cells. Cell Death Differ.

43. Guo Z, H Li, X Li, X Yu, H Wang, P Tang and N Mao. (2006). In vitro characteristics and in vivo immunosuppressive activity of compact bone-derived murine mesenchymal progenitor cells. Stem Cells 24:992-1000.

44. Phinney DG, G Kopen, RL Isaacson and DJ Prockop. (1999). Plastic adherent stromal cells from the bone marrow of commonly used strains of inbred mice: variations in yield, growth, and differentiation. J Cell Biochem 72:570-585.

45. Boregowda SV, V Krishnappa, JW Chambers, PV Lograsso, WT Lai, LA Ortiz and DG Phinney. (2012). Atmospheric oxygen inhibits growth and differentiation of marrow-derived mouse mesenchymal stem cells via a p53-dependent mechanism: implications for long-term culture expansion. Stem Cells 30:975-87.

46. Berniakovich I and M Giorgio. (2013). Low oxygen tension maintains multipotency, whereas normoxia increases differentiation of mouse bone marrow stromal cells. Int J Mol Sci 14:2119-34.

47. Yew TL, MC Chang, YT Hsu, FY He, WH Weng, CC Tsai, FY Chiu and SC Hung. (2013). Efficient expansion of mesenchymal stem cells from mouse bone marrow under hypoxic conditions. J Tissue Eng Regen Med 7:984-93.

48. Bonyadi M, SD Waldman, D Liu, JE Aubin, MD Grynpas and WL Stanford. (2003). Mesenchymal progenitor self-renewal deficiency leads to age-dependent osteoporosis in Sca-1/Ly-6A null mice. Proc Natl Acad Sci U S A 100:5840-5.

49. Ito CY, CY Li, A Bernstein, JE Dick and WL Stanford. (2003). Hematopoietic stem cell and progenitor defects in Sca-1/Ly-6A-null mice. Blood 101:517-23.

50. Psaltis PJ, S Paton, F See, A Arthur, S Martin, S Itescu, SG Worthley, S Gronthos and ACW Zannettino. (2010). Enrichment for STRO- 1 expression enhances the cardiovascular paracrine activity of human bone marrow- derived mesenchymal cell populations. J Cell Physiol 223:530-540.

51. Strioga M, S Viswanathan, A Darinskas, O Slaby and J Michalek. (2012). Same or not the same? Comparison of adipose tissue-derived versus bone marrow-derived mesenchymal stem and stromal cells. Stem Cells Dev 21:2724-52.

52. Hass R, C Kasper, S Bohm and R Jacobs. (2011). Different populations and sources of human mesenchymal stem cells (MSC): A comparison of adult and neonatal tissue-derived MSC. Cell Commun Signal 9:12.

53. Raicevic G, M Najar, B Stamatopoulos, C De Bruyn, N Meuleman, D Bron, M Toungouz and L Lagneaux. (2011). The source of human mesenchymal stromal cells influences their TLR profile as well as their functional properties. Cell Immunol 270:207-16.

54. Kronsteiner B, S Wolbank, A Peterbauer, C Hackl, H Redl, M van Griensven and C Gabriel. (2011). Human mesenchymal stem cells from adipose tissue and amnion influence T-cells depending on stimulation method and presence of other immune cells. Stem Cells Dev 20:2115-26.

55. Gronthos S, DM Franklin, HA Leddy, PG Robey, RW Storms and JM Gimble. (2001). Surface protein characterization of human adipose tissue-derived stromal cells. J Cell Physiol 189:54-63.

56. Festy F, L Hoareau, S Bes-Houtmann, AM Pequin, MP Gonthier, A Munstun, JJ Hoarau, M Cesari and R Roche. (2005). Surface protein expression between human adipose tissue-derived stromal cells and mature adipocytes. Histochem Cell Biol 124:113-21.

57. Kim YS, HJ Park, MH Hong, PM Kang, JP Morgan, MH Jeong, JG Cho, JC Park and Y Ahn. (2009). TNF-alpha enhances engraftment of mesenchymal stem cells into infarcted myocardium. Front Biosci (Landmark Ed) 14:2845-56.

FIGURE LEGENDS

Stem Cells and Development

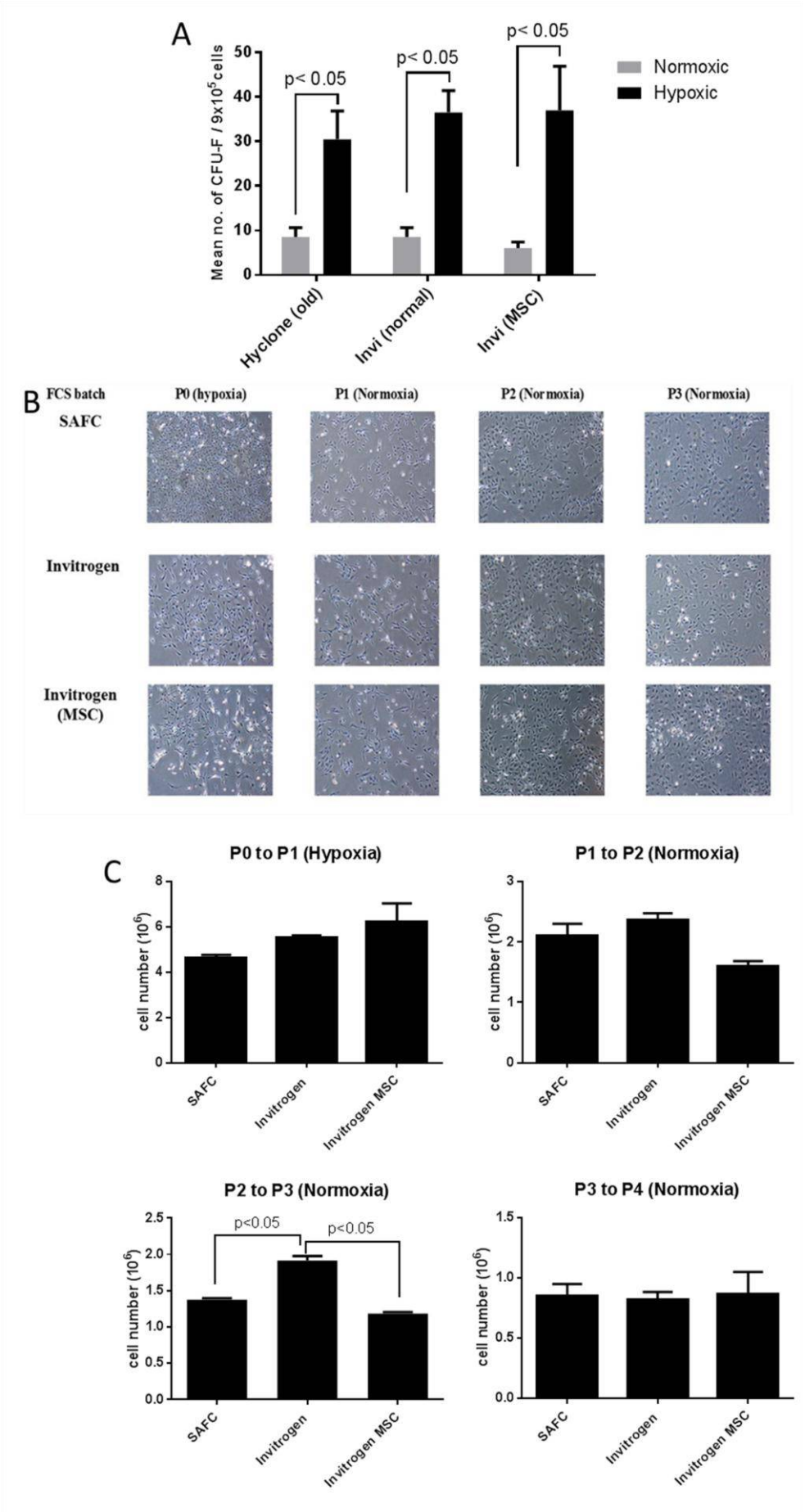

Figure 1. Optimization of CB mMSC isolation and culture conditions.

(A) CB depleted of bone marrow cells from C57BL/6 mice were digested with collagenase. CB cells were cultured in a 6-well plate at $9x10^5$ cells/well in 3ml primary MSC media containing 20% FBS from: **(1)** previously used FBS batch, **SAFC** (batch #10C126). Two new FBS serum batches tested include: **(2)** normal Invitrogen FBS, **Invitrogen** (batch #1153562) and **(3)** Invitrogen human MSC pre-screened FBS, **Invitrogen MSC** (batch #981394). The 6-well plates were cultured at either normal or under hypoxic (5% O_2, 10% CO_2, 85% N_2) conditions, 37^{o}C. The number of colony forming units fibroblast (CFU-F) between the different FBS batches were counted and compared. The figure indicates mean number of CFU-F per $9x10^5$ cells. **(B)** Morphology of mMSC examined in MSC media supplemented with the 3 different FBS batches. mMSC morphology was observed at the initial establishment of mMSC cell lines under hypoxia (Passage 0, P0) and subsequent sub-culturing of cells from P1 to P3. Any aberrant changes in mMSC morphology were examined under the different FBS batches (original magnification x100). The Nikon Eclipse Ti inverted microscope was used to capture images. **(C)** C57BL/6 mice mMSC progenitors or sub-cultured mMSC were seeded at either $3x10^4$ cells/cm^2 for P0 to P1 (hypoxia) or $1x10^4$ cells/cm^2 for P1 to P2, P2 to P3 and P3 to P4 (normoxia), respectively. At day 4 or 5 or confluency, mMSC were detached by trypsinization and the number of mMSC were counted. The figures indicate total mMSC yield cultured at P0 to P1 (under hypoxia) and P1 to P2, P2 to P3 and P3 to P4 (under normoxia). *$p<0.05$ vs. normoxia culture conditions **(A)** or vs. Invitrogen **(C)** was determined by one-way ANOVA with post-Sidak multiple comparison test. Error bars depict mean cell numbers of duplicate cell counts ± SD.

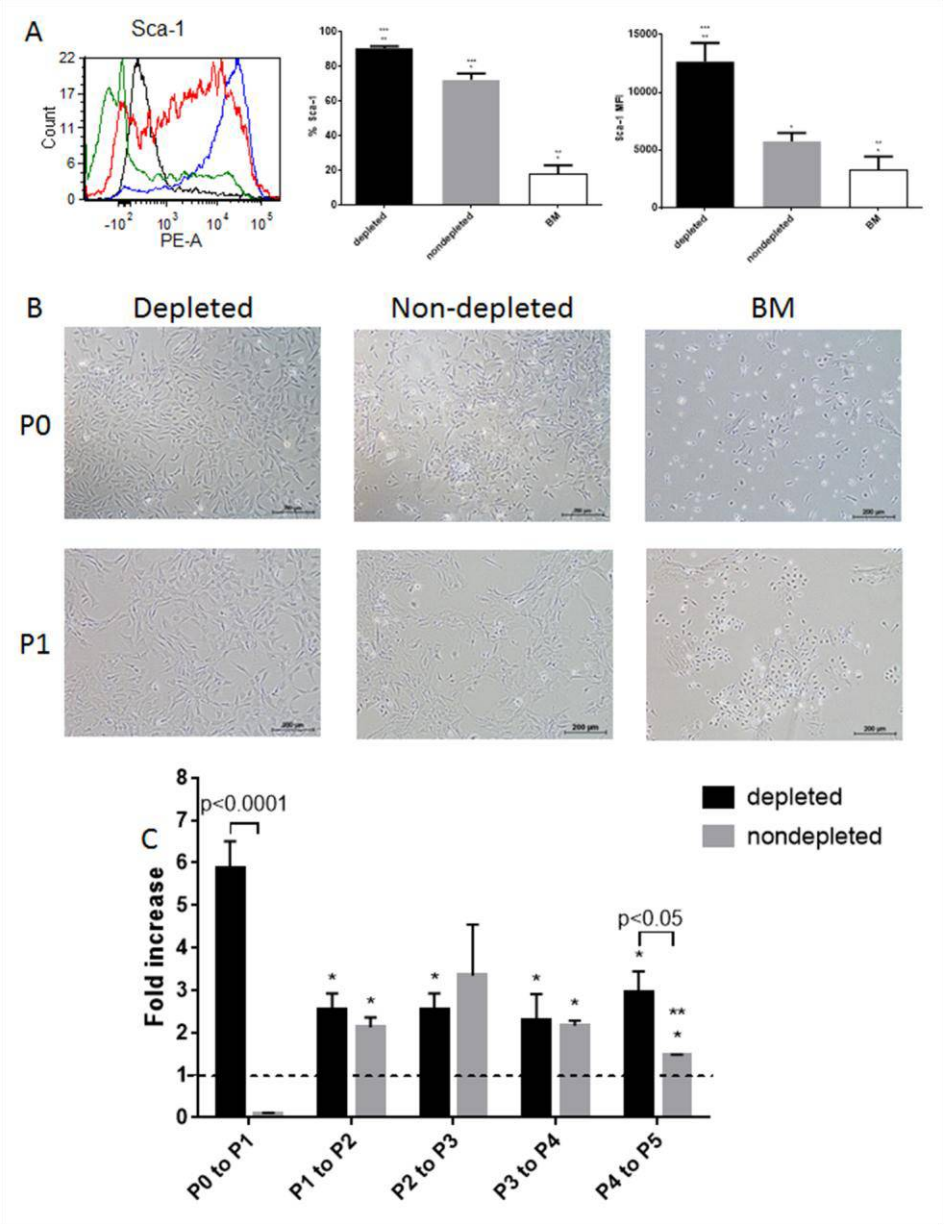

Figure 2. Enrichment of mMSC progenitors by CD45 and TER119 depletion of compact bones.

Bone marrow and compact bone (depleted and nondepleted) mMSC cell lines isolated from C57BL/6 mice were established under normoxia or hypoxia, respectively. CB nondepleted mMSC progenitors were obtained following collagenase digestion. CB depleted mMSC precursors were isolated by depleting CD45 and TER119 cells from the collagenase digested CB cell fraction. **(A)** Sca-1 surface marker expression of mMSC at Passage 1 (P1) was

assessed by flow cytometry. Histogram shows level of Sca-1 expression on mMSC and are depicted by the isotype control (black), depleted mMSC (blue), nondepleted mMSC (red) and BM mMSC (green). Data are one representative of 3 mMSC isolations. Graphs depict % Sca-1 positivity and Sca-1 mean fluorescence intensity (MFI). Data are pooled from 3 mMSC isolations. *p<0.05 vs. depleted, **p<0.05 vs. nondepleted, ***p<0.05 vs. BM determined by one-way ANOVA with post-Sidak multiple comparison test. **(B)** Morphology of BM, depleted and nondepleted mMSC at Passage 0 (P0) and 1 (P1). (original magnification x100). The Nikon Eclipse Ti inverted microscope was used to capture images. Data are one representative of 4 mMSC isolations. **(C)** Fold increase in depleted (black bars) and nondepleted (grey bars) MSC numbers calculated as harvest cell number divided by the initial seeding density number. At confluency, mMSC were detached by trypsinization and the numbers of mMSC were counted. The figures indicate total mMSC yield cultured at P0 to P1 (under hypoxia; n=4) and P1 to P2, P2 to P3, P3 to P4 and P4 to P5 (n=3 or 4, under normoxia). Data are pooled from 3 (nondepleted mMSC) or 4 (depleted mMSC) independent experiments with 3 or 4 mMSC donors. *p<0.05 for comparison of between individual mMSC groups (depleted or nondepleted) upon passaging (P0 to P5), **p<0.05 for comparison of nondepleted mMSC (P4 to P5) vs. all other nondepleted mMSC passages. p<0.05 of depleted vs. nondepleted mMSC are indicated on the graph. Statistical significances were determined by two-way ANOVA with post-Sidak multiple comparison test**. (A,C)** Error bars depict means of ± SEM of triplicates or quadruplicates.

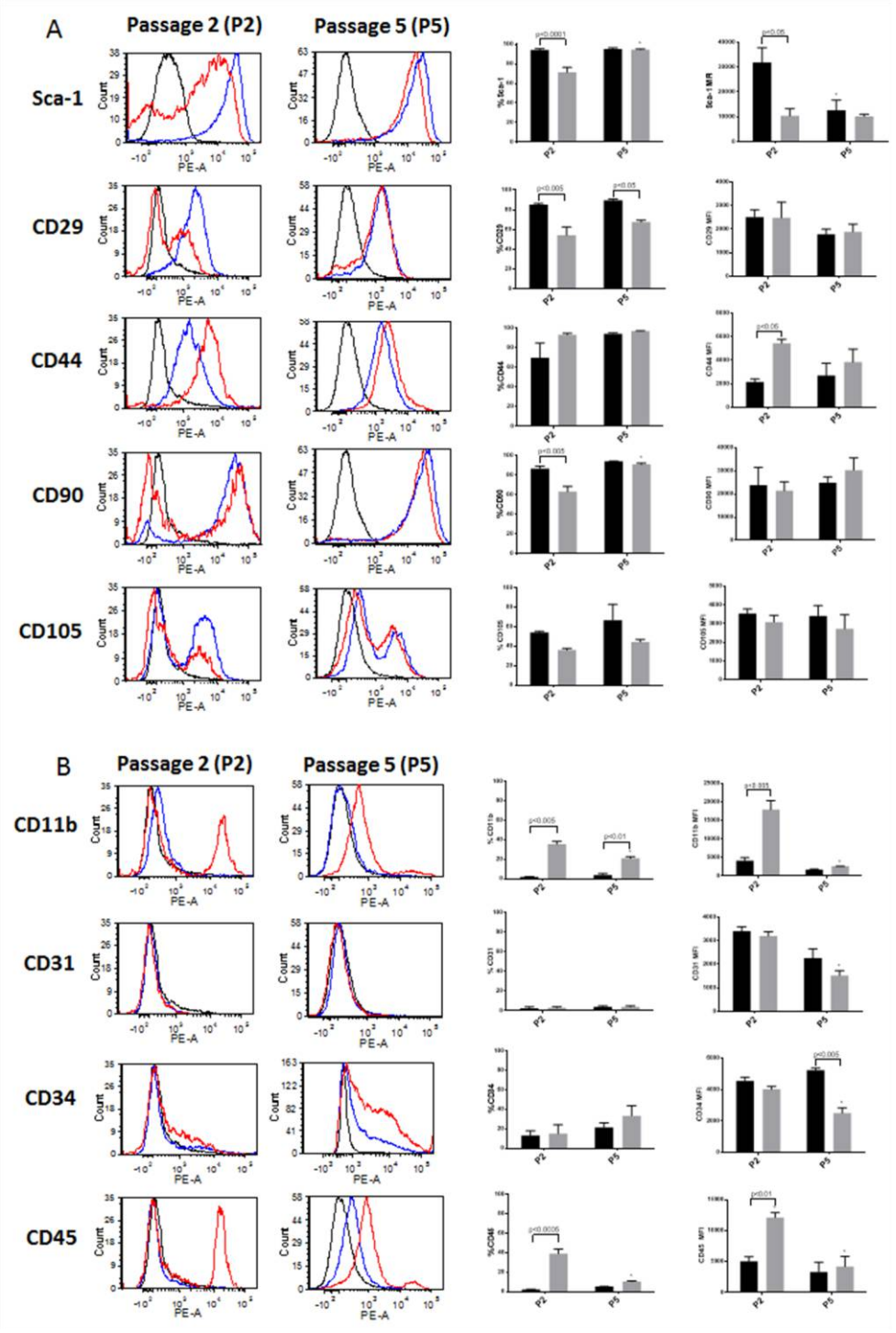

Figure 3. Immunophenotype comparison of compact bone depleted and nondepleted mMSC.

The expression of standard positive **(A)** and negative **(B)** MSC cell surface markers were assessed by flow cytometry at early (Passage 2, P2) and late (P5) cell passages in depleted

and nondepleted CB mMSC. Histograms show level of surface marker expression on mMSC and are depicted by the isotype control (black), depleted mMSC (blue) and nondepleted mMSC (red). Data are one representative of 3 mMSC isolations. Graphs depict % positivity and mean fluorescence intensity (MFI). Data are pooled from 3 mMSC isolations. *$p<0.05$ for P2 vs. P5 between individual mMSC (depleted or nondepleted) comparison groups. $p<0.05$ of depleted vs. nondepleted mMSC are indicated on the graphs. Error bars depict means of ± SEM of triplicates or quadruplicates.

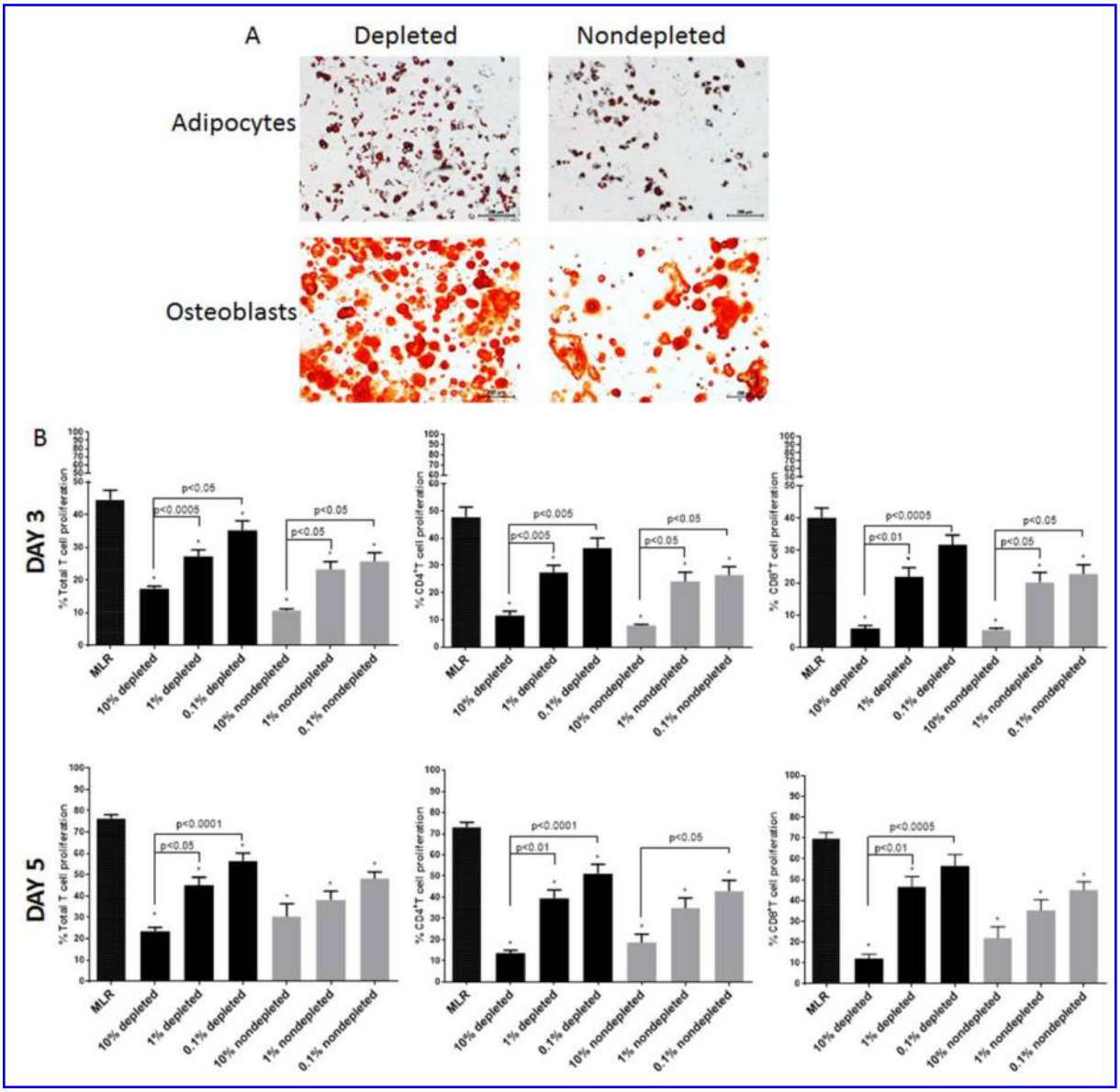

Figure 4. Depleted and nondepleted mMSC inhibit allogeneic T cell proliferation in a dose-dependent manner.

(A) Functional differentiation of depleted and nondepleted mMSC into adipocytes (Oil red stained fat; original magnification x100) and osteoblasts (Alizarin red stained mineral; original magnification x100) for 4 weeks. The Nikon Eclipse Ti inverted microscope was used to capture images. Representative of 1 of 3 mMSC isolations. **(B)** Depleted or nondepleted CB mMSC were co-cultured with CFSE-labelled $CD3^+$ T cells (C57BL/6 mice) allo-stimulated by irradiated DC (BALB/c mice) at 10% UT-MSC, 1% UT-MSC and 0.1%

UT-MSC. At 3- or 5- days, T cells were isolated and cell-surface stained with anti-mouse CD4 and anti-mouse CD8 and acquired on BD FACSCanto II. Percentage of total, $CD4^+$ and $CD8^+$ T cell proliferation was determined and represented in the graphs. MLR in the absence of mMSC indicates maximal T cell proliferation. Data are pooled from 9 (depleted mMSC) and 4 (nondepleted mMSC) independent experiments. *$p<0.05$ vs. MLR determined by Kruskal-Wallis with post-Dunn multiple comparison test. Error bars depict means of ± SEM.

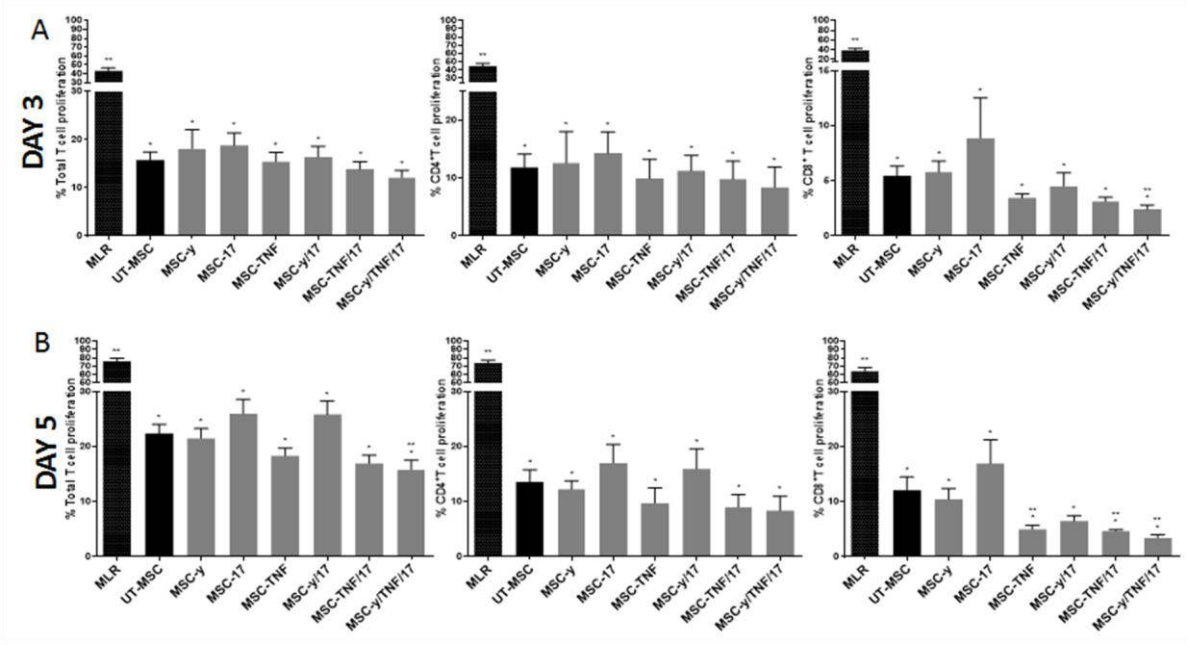

Figure 5. TNF-α enhanced mMSC suppression of T cell proliferation.

CB depleted mMSC were either untreated (**UT-MSC**) or treated for 5 days with single recombinant cytokines: IFN-γ (**MSC-γ**), IL-17A (**MSC-17**) and TNF-α (**MSC-TNF**); or in a cytokine combination cocktail: IFN-γ and IL-17A (**MSC-γ/17**); TNF-α and IL-17A (**MSC-TNF/17**); or IFN-γ, TNF-α and IL-17A (**MSC-γ/TNF/17**). Mouse MSC were co-cultured with CFSE-labelled $CD3^+$ T cells (C57BL/6 mice) allo-stimulated by irradiated DC (BALB/c mice) at a 10% mMSC dose. At 3- **(A)** or 5- **(B)** days, T cells were isolated and cell-surface stained with anti-mouse CD4 and anti-mouse CD8 and acquired on BD FACSCanto II. Percentage of total, $CD4^+$ and $CD8^+$ T cell proliferation was determined and represented in the graphs. MLR in the absence of mMSC indicates maximal T cell proliferation. Data are pooled from 6 (MLR, UT-MSC, MSC-17) and 3 (MSC-γ, MSC-TNF, MSC-γ/17, MSC-TNF/17, MSC-γ/TNF/17) independent experiments. *$p<0.05$ vs. MLR determined by Kruskal-Wallis with post-Dunn multiple comparison test. Error bars depict means of ± SEM.

TABLES

Table 1 Mouse MSC antibody panel

Antibody	Clone	Fluorochrome	Company
MSC phenotyping:			
Sca-1	D7	PE	eBioscience
CD29	265917	PE	R&D systems
CD90 / Thy1	778053	PE	R&D systems
CD105	MJ7/18	PE	eBioscience
CD31	390	PE	eBioscience
CD34	MEC14.7	PE	Biolegend
CD44	IM7	PE	eBioscience
CD11b	M1/70	PE	eBioscience
CD45	30-F11	PE	eBioscience
IL-17RA	PAJ-17R	PE	eBioscience
IL-17RC	Leu21-Trp465	APC	R&D Systems
Isotype controls			
Rat IgG2a	eBR2a	PE	eBioscience
Rat IgG2b	eB149/10H5	PE	eBioscience
Rat IgG1	eBRG1	APC	eBioscience
Armenian Hamster IgG	eBio299Arm	PerCP-Cy5.5	eBioscience
Rat IgG2a	RTK2758	BV421	Biolegend
T cells			
CD4	GK1.5	APC-eFluor	eBioscience
CD8	53-6.7	Pe-Cy7	eBioscience

Table 2 Optimization of collagenase digestion of compact bones of C57BL/6 mice

	[Collagenase] (mg/ml)	Digestion time (hr)	Yield (x10^5 cells)	% Sca-1^+ cells	Mean CFU-F
Collagenase I	3	1	9	2.47	59
Collagenase II	1	1	7.95	8.69	36
Collagenase II	1	2	5.2	11.09	78
Collagenase II	3	1	10.3	34.66	80
Collagenase II	3	2	13.25	2.08	55

CB cell yield immediately after CB digestions and the % Sca-1^+ cells were determined. Yield of cells was counted as the number of CB cells released immediately after CB digestion.

Table 3 Mouse MSC culture condition optimization: normoxia vs. hypoxia

	Mean CFU-F	
	Normoxia	**Hypoxia**
Compact bones cells	5	51
Bone marrow cells	0	1

Table 4. Cumulative data on CB depleted and nondepleted mMSC suppression of T cell proliferation

	% proliferation ± SEM (experimental replicates)						
		Depleted			**Nondepleted**		
T cell subsets	MLR (n=9)	10% dep (n=9)	1% dep (n=9)	0.1% dep (n=4)	10% nondep (n=4)	1% nondep (n=4)	0.1% nondeep (n=4)
DAY 3 MLR							
Total T cells	44.53 ± 2.944	**17.27 ± 0.8663**	**27.24 ± 1.946**	**35.20 ± 2.841**	**10.61 ± 0.5909**	**23.38 ± 2.382**	**25.75 ± 2.559**
$CD4^+$ T cells	47.91 ± 3.568	**11.63 ± 1.513**	**27.45 ± 2.625**	36.47 ± 3.613	**7.94 ± 0.3606**	**24.15 ± 3.348**	**26.42 ± 3.128**
$CD8^+$ T cells	40.17 ± 2.950	**6.01 ± 0.8293**	**21.90 ± 2.866**	31.79 ± 2.974	**5.41 ± 0.6710**	**20.20 ± 3.045**	**22.80 ± 2.835**
DAY 5 MLR							
Total T cells	**76.47 ± 1.645**	**23.49 ± 1.863**	**45.15 ± 3.639**	**56.53 ± 3.684**	**30.31 ± 5.991**	**38.26 ± 3.994**	**48.15 ± 3.085**
$CD4^+$ T cells	73.15 ± 2.203	**13.74 ± 1.252**	**39.54 ± 3.921**	**51.31 ± 4.366**	**18.73 ± 3.910**	**34.92 ± 4.741**	**42.85 ± 5.221**
$CD8^+$ T cells	69.65 ± 3.046	**12.14 ± 2.151**	**46.56 ± 4.930**	56.58 ± 5.575	**21.91 ± 5.478**	**35.36 ± 5.002**	**45.02 ± 4.006**

0.1%, 1% or 10% depleted (dep) and nondepleted (nondep) UT-mMSC were co-cultured with $CD11c^+$ mDC stimulated $CD3^+$ T cells for 3 or 5 days. $CD4^+$ and $CD8^+$ T cell proliferation was measured in a one-way MLR. Data are presented as percentage $CD4^+$ and $CD8^+$ T cell

proliferation. Bold fonts indicate $p<0.05$ vs. MLR determined by Kruskal-Wallis with post-Dunn multiple comparison test. Error bars depict means of ± SEM.

SUPPLEMENTARY FIGURE LEGENDS

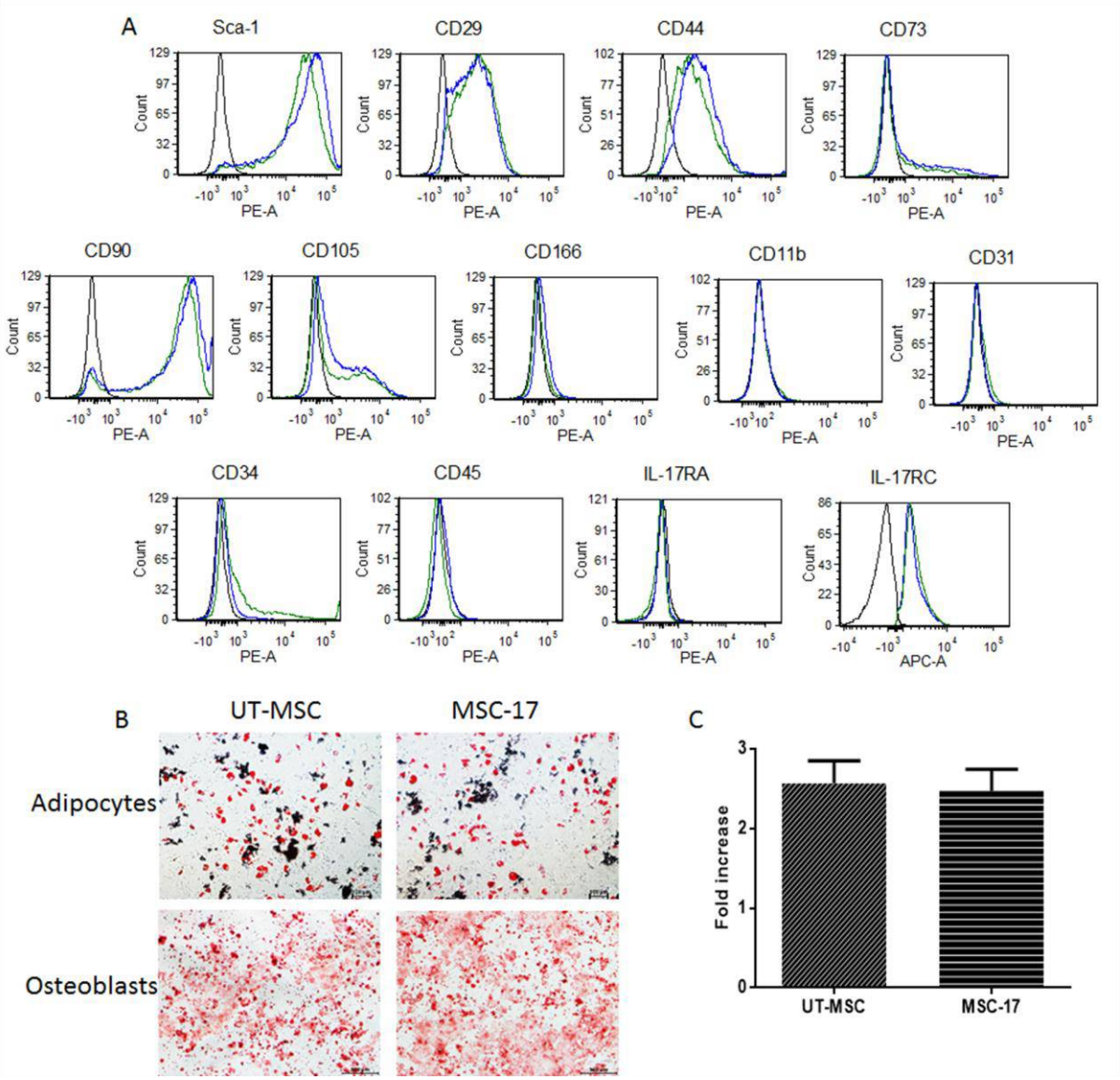

Figure S1. Characterisation of UT-mMSC and mMSC-17.

Compact bones derived mMSC isolated from C57BL/6 mice were either untreated (UT-mMSC) or treated with IL-17A (MSC-17) for 5 days. **(A)** The expression of surface markers on mMSC was assessed by flow cytometry. The histograms show levels of surface marker expression on mMSC and are depicted by the isotype control (black), UT-MSC (green) and MSC-17 (blue). Data are one representative of 4 mMSC isolations. **(B)** Functional

differentiation of mMSC into adipocytes (Oil red stained fat; original magnification x100) and osteoblasts (Alizarin red stained mineral; original magnification x100) for 4 weeks. The Nikon Eclipse Ti inverted microscope was used to capture images. Representative of 1 of 3 mMSC isolations. **(C)** Fold increase in mMSC numbers calculated as harvest cell number divided by the initial seeding number. Cell numbers were determined by trypan blue exclusion assay. Data are pooled from 4 independent experiments of 4 mMSC isolations. *p< 0.05 versus UT-MSC was determined by two-way ANOVA with post-Sidak multiple comparison test. Error bars depict mean ± SEM.

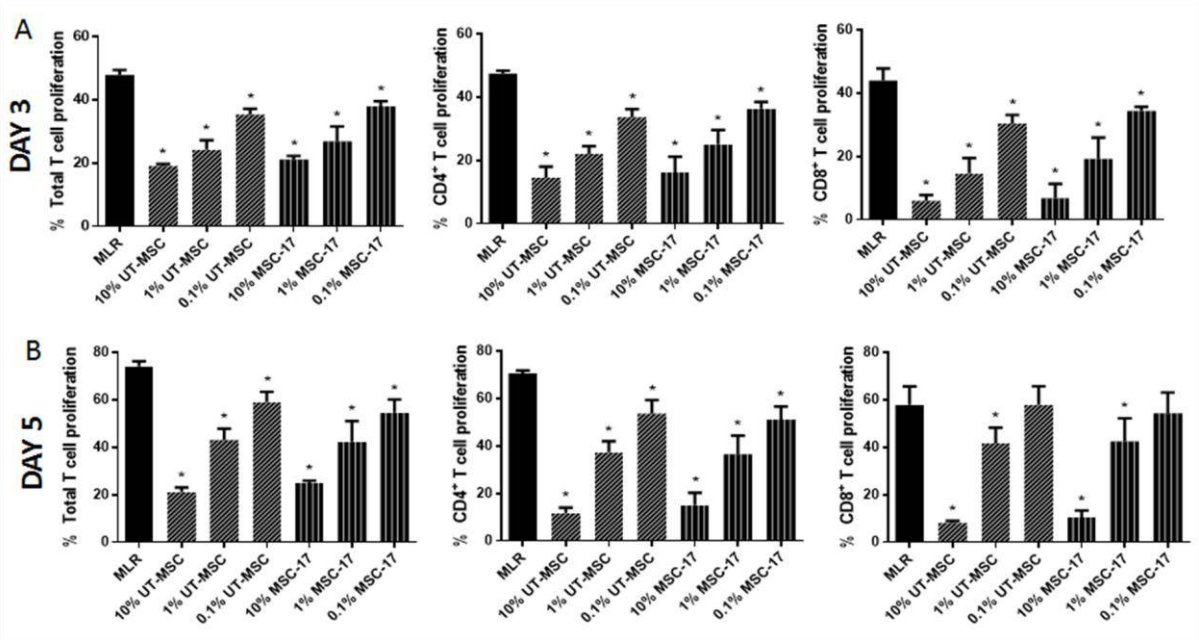

Figure S2. IL-17A does not enhance mMSC suppression of T cell proliferation.

UT-MSC or mMSC treated for 5 days with IL-17A were co-cultured with CFSE-labelled $CD3^+$ T cells (C57BL/6 mice) allo-stimulated by irradiated DC (BALB/c mice) at 10%, 1% and 0.1% mMSC doses. At **(A)** 3- or **(B)** 5- days, T cells were isolated and cell-surface stained with anti-mouse CD4 and anti-mouse CD8 and acquired on BD FACSCanto II. Percentage of total, $CD4^+$ and $CD8^+$ T cell proliferation was determined and represented in the graphs. MLR in the absence of mMSC indicates maximal T cell proliferation. Data are pooled from 3 independent experiments. *$p<0.05$ vs. MLR determined by two-way ANOVA with post-Sidak multiple comparison test. Error bars depict means of triplicates ± SEM.

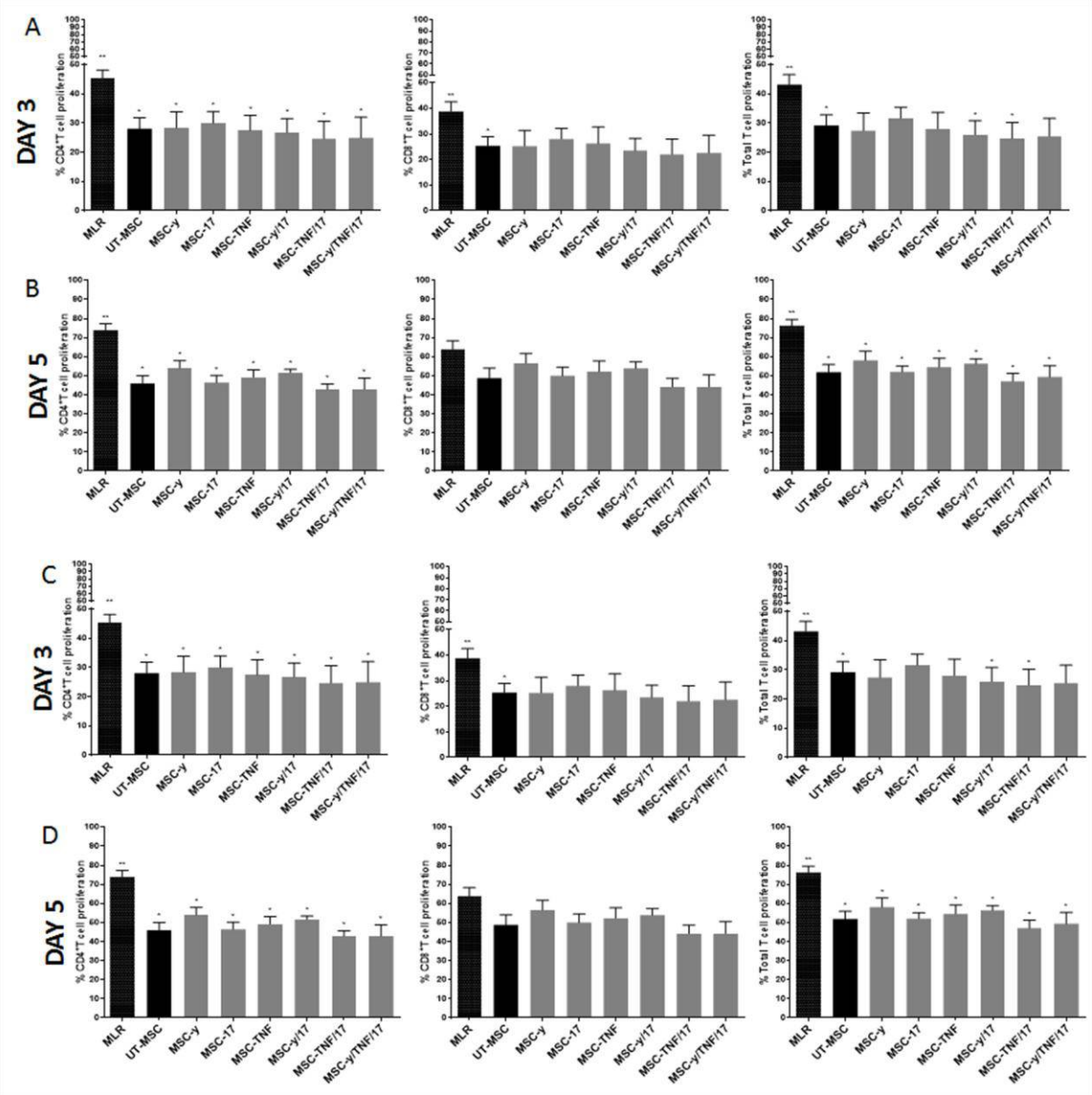

Figure S3. TNF-α does enhance not mMSC suppression of T cell at low doses.

CB depleted mMSC were either untreated (**UT-MSC**) or treated for 5 days with single recombinant cytokines: IFN-γ (**MSC-γ**), IL-17A (**MSC-17**) and TNF-α (**MSC-TNF**); or in a cytokine combination cocktail: IFN-γ and IL-17A (**MSC-γ/17**); TNF-α and IL-17A (**MSC-TNF/17**); or IFN-γ, TNF-α and IL-17A (**MSC-γ/TNF/17**). Mouse MSC were co-cultured with CFSE-labelled $CD3^+$ T cells (C57BL/6 mice) allo-stimulated by irradiated DC (BALB/c mice) at 1% **(A,B)** or 0.1% **(C,D)** mMSC doses. At 3- **(A,C)** or 5- **(B,D)** days, T cells were

isolated and cell-surface stained with anti-mouse CD4 and anti-mouse CD8 and acquired on BD FACSCanto II. Percentage of total, $CD4^+$ and $CD8^+$ T cell proliferation was determined and represented in the graphs. MLR in the absence of mMSC indicates maximal T cell proliferation. Data are pooled from 6 (MLR, UT-MSC, MSC-17) and 3 (MSC-γ, MSC-TNF, MSC-γ/17, MSC-TNF/17, MSC-γ/TNF/17) independent experiments. *$p<0.05$ vs. MLR determined by Kruskal-Wallis with post-Dunn multiple comparison test. Error bars depict means of ± SEM.